

LETTER

Open Access



Multi-height micropylramids based pressure sensor with tunable sensing properties for robotics and step tracking applications

Dongik Oh^{1†}, Jungyeon Seo^{1†}, Hang Gyeom Kim¹, Chaehyun Ryu¹, Sang-Won Bang¹, Sukho Park^{1,2} and Hoe Joon Kim^{1,2*} 

Abstract

Precise sensing of pressure is essential for various mechanical and electrical systems. The recent emergence of flexible pressure sensors has enabled novel applications, such as human–machine interfaces, soft robotics, and wearable devices. Specifically, the piezoresistive sensing scheme is widely adapted for flexible pressure sensors as it is simple and exhibits outstanding measurement sensitivity and stability. The sensing properties of piezoresistive pressure sensors mainly depends on the materials and contact morphologies at the interface. This paper proposes a flexible pressure sensor based on multi-height microstructures in which the measurement sensitivity and detection range are tunable. Such tunability is due to the sequential contact of micropylramids with different heights. The multi-height micropylramid structured PDMS layer with stamp-coated multi-walled carbon nanotubes (MWCNTs) acts as a conductive active layer and a gold interdigitated electrode (IDE) patterned polyimide (PI) layer works as the bottom electrode. The fabricated sensor exhibits a sensitivity of 0.19 kPa^{-1} , a fast response speed of 20 ms, and a detection range of up to 100 kPa. The sensor is applied to a robotic gripper for object recognition and integrated into a shoe to track walking motions.

Keywords: Flexible pressure sensor, Piezoresistive, Multi-height, Carbon nanotubes, Robotic sensor

Introduction

The flexible and wearable pressure sensors have drawn much attention as they can detect various biomechanical motions, actuation of mechanical systems, and environmental factors [1–4]. Owing to their thin structure and soft body, flexible pressure sensors exhibit high measurement sensitivities, which is enough to detect human pulse and vocal cord vibrations [5]. Recently, the emergence of durable and high-sensing range pressure sensors has enabled the development of pressure sensor

integrated robotic systems and wearable devices. Such pressure sensors mimic human sensory systems and can realize sophisticated human–robot interfaces and electronic skins.

Among various sensing mechanisms, piezoresistive sensors possess advantages such as high durability, a simple setup, and a wide range of materials selection [6–9]. In piezoresistive sensors, the pressure-dependent change in the contact area of conducting microstructures induces a shift in electrical resistance [10–13]. The material and morphology of microstructures decide the sensor properties, such as sensitivity and detection range. Various microstructures of porous structures, microdomes, micropylramids, and microfibers, have proved the measurement sensitivity of pressure sensors [12, 14–19]. Fabrication of microstructures using template molding allows a rapid and straightforward fabrication [17, 20,

[†]Dongik Oh and Jungyeon Seo author contributed equally to this work

*Correspondence: joonkim@dgist.ac.kr

¹ Department of Robotics and Mechatronics Engineering, Daegu Gyeongbuk Institute of Science & Technology (DGIST), 333, Techno jungang-daero, Hyeonpung-eup, Dalseong-gun, Daegu 42988, Republic of Korea
Full list of author information is available at the end of the article

21]. Researchers have used sandpapers, lotus leaves, and etched silicon wafers as molds to create microstructures [17, 18, 20–25]. In most cases, the detection range is inversely proportional to the sensitivity, limiting the use of flexible pressure sensors to only a few kPa ranges [17, 21, 23, 25]. In addition, many studies adopt microstructures with identical designs and the effect of using multi-height microstructures are not well understood.

This study presents a multi-height micropyramid-based pressure sensor to adjust the sensitivity and detection range. For mold fabrication, potassium hydroxide (KOH) wet etching of silicon with different openings generates micropyramid cavities with different heights and base

widths. The developed piezoresistive pressure sensors consist of microstructures of up to three different sizes or heights and analyzed their sensing properties. The sensors are applied to step tracking and integrated onto a robotic gripper system, showcasing a possible application area of the presented multi-height pressure sensor.

Materials and methods

Mold and pressure sensor fabrication

Figure 1a shows the fabrication process of KOH etched silicon mold with multi-height micropyramid structures. Initially, the 6-inch $\langle 100 \rangle$ silicon wafer with 200 nm of silicon nitride (Si_3N_4) is prepared by plasma-enhanced

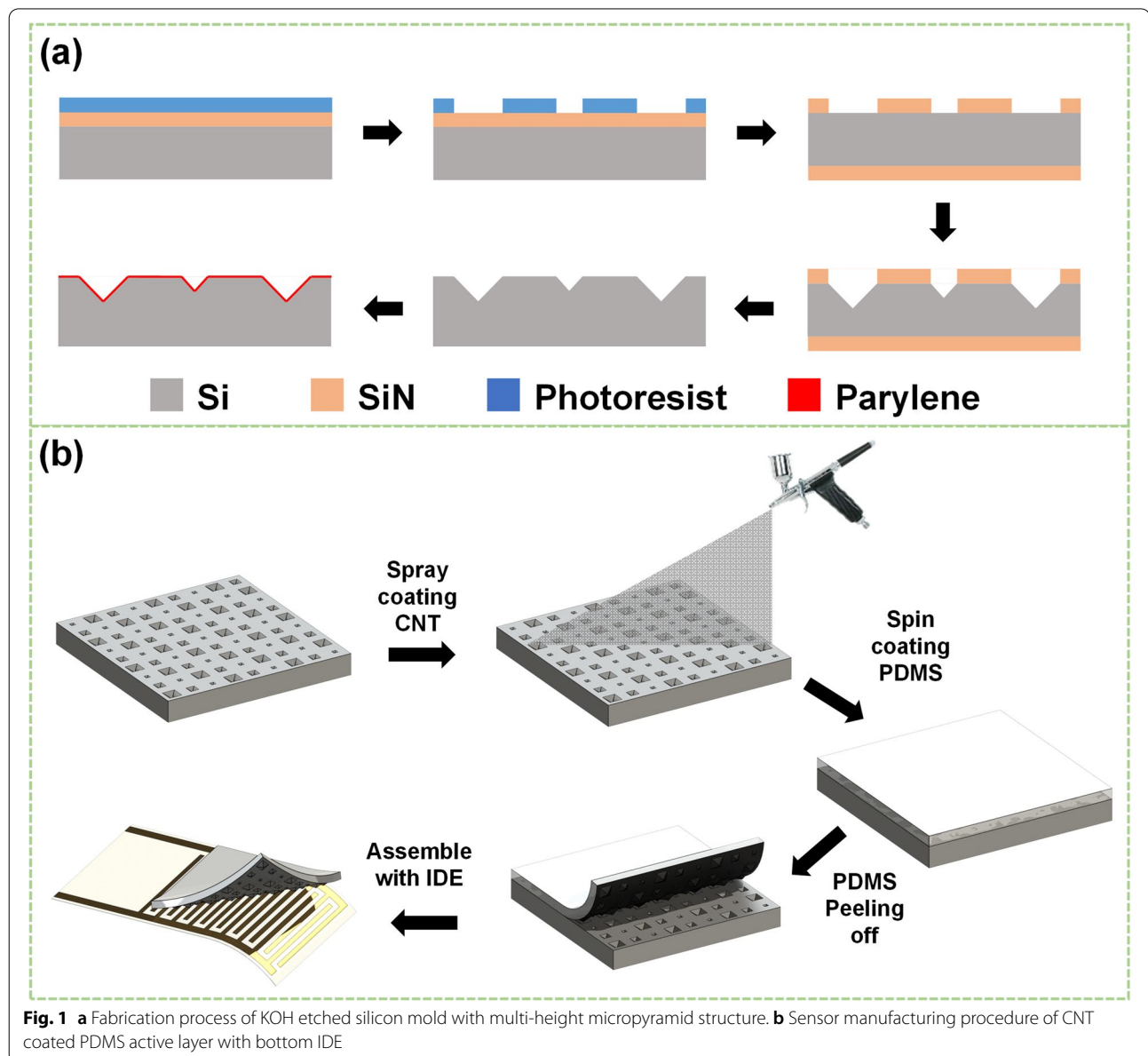


Fig. 1 **a** Fabrication process of KOH etched silicon mold with multi-height micropyramid structure. **b** Sensor manufacturing procedure of CNT coated PDMS active layer with bottom IDE

chemical vapor deposition (PECVD). The photolithography process is used to pattern the photoresist (AZ GXR 601), and then reactive ion etching (RIE) is performed to make a Si_3N_4 mask for KOH etching. After the PR removal using acetone, a 200 nm-thick Si_3N_4 is PECVD deposited on the backside of the wafer to protect the wafer from KOH wet etching. KOH anisotropic etching is processed for 36 min to make a maximum 42.4 μm height (h) of micropyramid structure (60 μm of bottom width, w) followed by a buffered oxide etch (BOE) to remove Si_3N_4 . By controlling the size of the opening, the final height of micropyramids can be adjusted. Finally, the multi-height micropyramid structure patterned silicon wafer is coated with parylene-C to lower the adhesion of PDMS during the molding and peeling process.

Figure 1b shows the pressure sensor manufacturing process. CNT is spray-coated on the fabricated silicon mold for 100 s (0.5 wt.% MWCNT in IPA, Outer diameter: 5~15 nm, length: 50 μm) at a rate of 0.15 mL/sec. The distance of 30 cm between the spray nozzle and the sensor substrate ensures the formation of a highly uniform CNT layer. Then, a PDMS mixture solution (Sylgard 184, base: agent=10: 1) is spin-coated at 300 rpm two times, followed by a 30 min vacuum treatment to enhance the adhesion between CNT and PDMS. After curing the PDMS at 150 $^\circ\text{C}$ for 10 min, the PDMS/CNT layer detached from a Si mold, forming a conducting active layer. Unlike the conventional spray-coating

CNTs on the substrate, the proposed process spray-coats CNTs before PDMS casting and curing. We define such a method as stamp-coating. The bottom interdigitated electrode (IDE) was fabricated on a polyimide (PI, VTEC 1388) tape by the photolithography and liftoff process. The electrode consists of a 10 nm Cr adhesion layer and a 100 nm Au. The size of a sensor is $1 \times 1 \text{ cm}^2$.

Device characterization and experiment

For materials and device characterization, a Raman spectrum (Nanobase XPER RF) study was performed and scanning electron microscopy (SEM, Hitachi S 4800) analyses. Au wires were soldered to the end of IDE contacts to form electrical connections to the sensor. The electrical resistance of the sensor is monitored using a digital multimeter (Agilent 34401A) connected to a PC with a LabView program. A universal testing machine (UTM) is used for loading and durability measurements. All measurements were taken under ambient conditions of atmospheric pressure and temperature of 25 $^\circ\text{C}$.

Results and discussion

Figure 2a–e show the SEM micrographs of the fabricated micropyramids with different designs. The proposed molding method results in micropyramids of various sizes and a sharp tip. Figure 2a shows the pristine PDMS micropyramids of identical size and height. Figure 2b–d show the various dimensions of PDMS

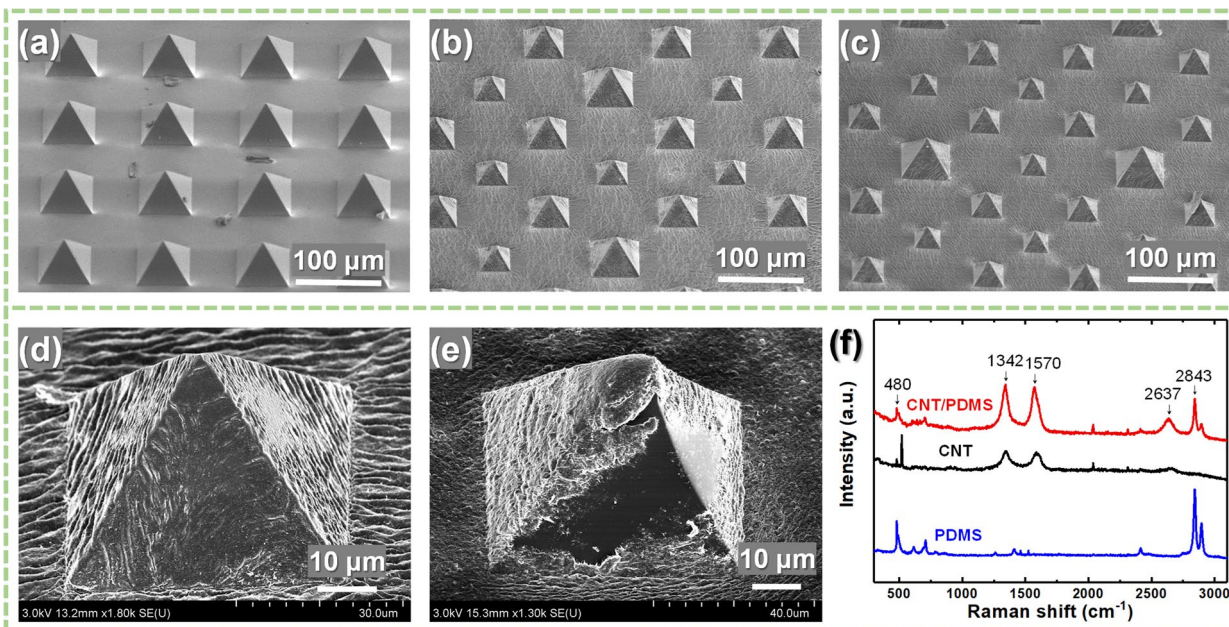


Fig. 2 SEM micrographs of the (a) bare PDMS micropyramid, CNT-coated PDMS micropyramids with (b) 2 different heights and (c) 3 different heights, micropyramids with a (d) stamp-coated CNT layer and (e) spray-coated CNT layer. f Raman spectrum of PDMS, pristine CNT, and CNT-coated PDMS

micropylamids with CNT coated using the proposed stamp-coating method. As the layer of CNT is coated on the mold before the PDMS curing, it is clear that CNT makes good and conformal adhesion to PDMS micropylamids. In addition, the tip of the micropylamid is fully covered with CNT using this method. In contrast, the conventional method of spray-coated CNTs on PDMS microstructures resulted in peeling and nonuniform surface coverage, as shown in Fig. 2e. Thus, the proposed stamp-coating method of CNT on PDMS is robust and adequate to form conducting layers on 3D microstructures. A Raman study is performed to validate that the presented fabrication method does not degrade the quality of CNTs. Figure 2f shows the acquired Raman spectra of PDMS, pristine CNT before coating, and CNT/PMDS composite film. The measured Raman peaks of PDMS and CNT follow the reported values. The CNT/PMDS composite also shows representative peaks of CNT (D-peak, G-peak, 2D-peak) and PDMS. The measured D-peak to G-peak intensities is 1.030 and 1.038 for the pristine CNT and CNT/PMDS composite.

Figure 3a shows the working principle of the multi-height micropylamid flexible pressure sensor. At the initial state, only the tip of the tallest micropylamids

makes contact with the bottom electrode. When pressure is applied, the contact area of the taller micropylamid increases, resulting in a decrease in the sensor's electrical resistance. As the applied pressure increases, the smaller micropylamids contact the bottom electrode. Such a sequential contact mechanism allows a wide range of pressure sensing and improvement in measurement sensitivity. Table 1 shows the design parameters of fabricated multi-height micropylamids-based pressure sensors. In this work, up to 3 different sizes of micropylamids with based widths (w) of 18, 36, and 60 μm are studied. For the sensor with single-height micropylamids, the w of the micropylamid is 60 μm . The sensor with two and three

Table 1 Design of studied multi-height micropylamids based pressure sensor

No. of different micropylamid sizes	No. of Microstructures (per cm^2)			Initial resistance(Ω)
	$w = 60 \mu\text{m}$	$w = 36 \mu\text{m}$	$w = 18 \mu\text{m}$	
1	6161	–	–	591
2	5776	–	5776	1464
3	1369	5476	4107	2180

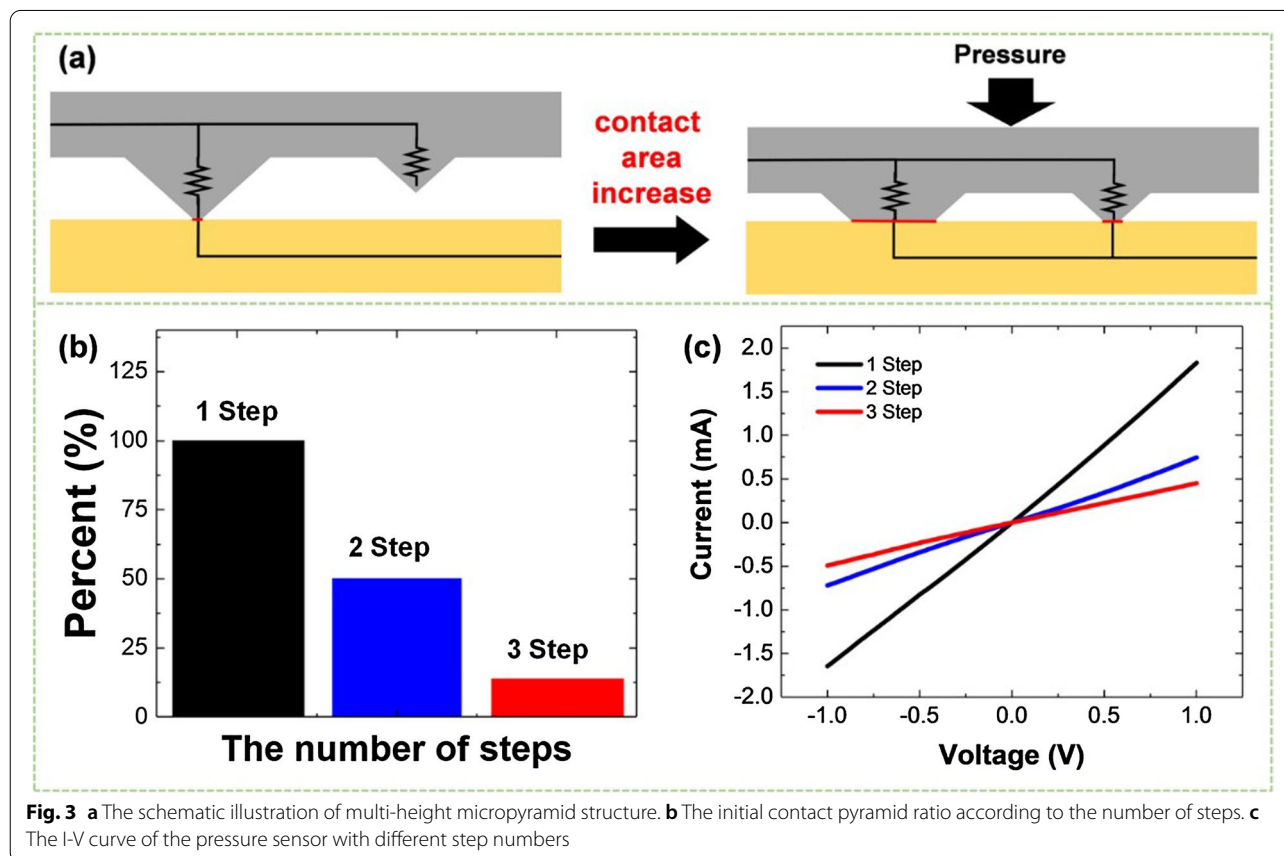


Fig. 3 **a** The schematic illustration of multi-height micropylamid structure. **b** The initial contact pyramid ratio according to the number of steps. **c** The I-V curve of the pressure sensor with different step numbers

different micropyramids heights is designed to have the micropyramids of $w=18, 60 \mu\text{m}$, and $w=18, 36$, and $60 \mu\text{m}$, respectively.

Since the developed sensor consists of multi-height micropyramids, only the tallest micropyramids make contact when no pressure is applied, as shown in Fig. 3b. The sensor's electrical resistance without an applied pressure decreases as the number of the tallest micropyramids decreases. Figure 3c shows the I–V curve of the unloaded sensor and the measured resistance of 2180, 1464, and 591Ω for 3-step, 2-step, and 1-step sensors, respectively. The linear I–V relation confirms a conformal and stable electrical contact between the CNT/PDMS active layer and bottom IDE.

The compression test is conducted over the pressure range from 0 to 100 kPa to analyze the piezoresistive response of the pressure sensor. Figure 4a shows the resistance change under varying pressure of each sensor. The measurement sensitivity, a %change in sensor resistance divided by applied pressure up to 66.7% of saturation value, is 0.0075 kPa^{-1} , 0.030 kPa^{-1} , 0.165 kPa^{-1} . The detection range defined as the point where sensor response reaches 90% of the saturation value is 23.8 kPa, 13.2 kPa, and 3.5 kPa for 1, 2, and 3-step sensors. From this, it can be concluded that both the measurement sensitivity and detection range can be tuned by adjusting the size and composition of multi-height micropyramids.

Such unique characteristics allow building of a flexible pressure sensor with adjustable sensing properties for target sensing applications. Figure 4b shows the resistance response of the 3-step pyramid pressure sensor with different size compositions. The sensitivity is 0.084 kPa^{-1} , and the detection range is 7.6 kPa for the 60, 54, and $48 \mu\text{m}$ pyramid composition: the sensitivity increases but the detection range decreases as the size composition changes. Thus a fine-tuning of sensing performances of the multi-height sensor is possible by using different size compositions of micropyramids.

The sensor response is monitored at three different applied pressures, 2, 3.3, and 13 kPa, to verify the sensor performance under varying loads, as shown in Fig. 4c. The results show that the developed sensor can track changes in pressure and reach a stable output under a consistent loading. Response and recovery duration is also essential parameter for pressure sensors. Figure 4d shows a response of the sensor under pulsed loading by human touch. The response time is measured to be 20 ms, and the recovery time was 40 ms. The sampling time was limited to 10 ms due to the experiment conditions, but the developed sensor can track rapid changes in applied pressure. Figure 4e shows the result of the durability test of 2500 cycles of loading at 2 kPa at a rate of 1.25 cycles/sec. The cyclic test shows no drift in the sensor response, showing that the presented sensor is robust and suited

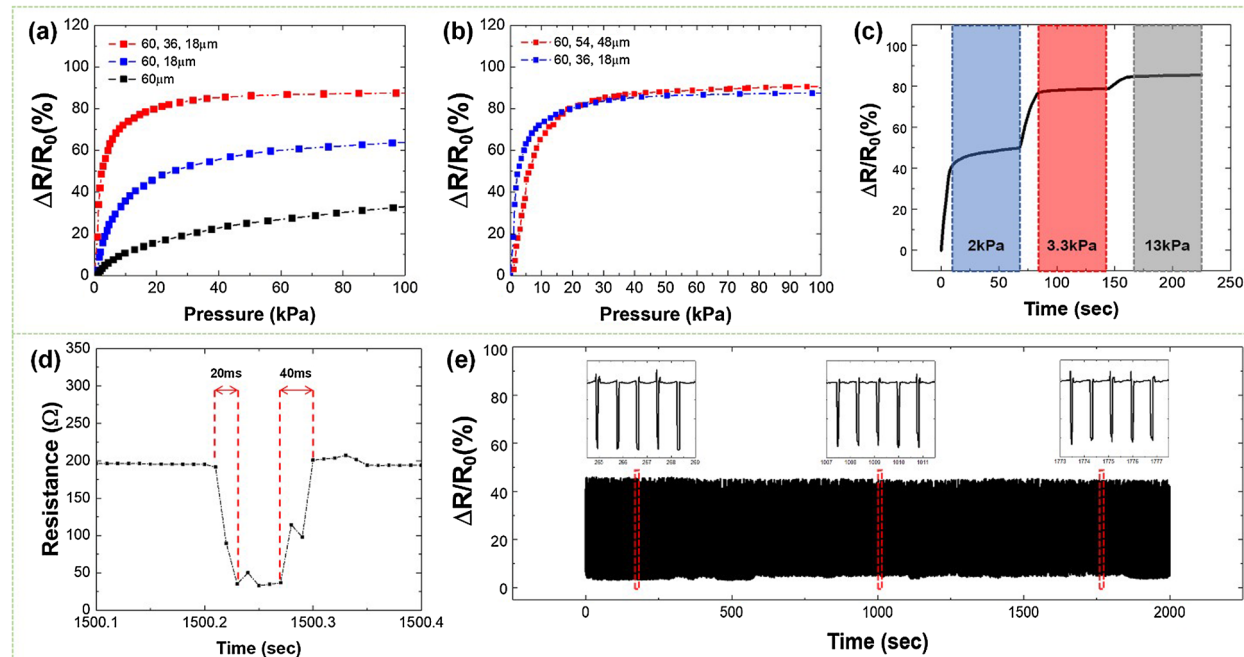


Fig. 4 **a** The resistance response of the sensor with a different number of steps. **b** The resistance response of 3 step pyramid pressure sensor with different height compositions. **c** Compression maintenance test at the applied pressures of 2, 3.3, and 13 kPa. **d** Response and recovery performance of the sensor. **e** Durability test under 2500 cyclic loading at 2 kPa

for prolonged operation in various circumstances. In addition, there was no visual damage to the sensor after such a lengthy operation.

The developed multi-height pressure sensor is used for various applications. Figure 5a–c shows the pressure sensor attached robotic gripper with two fingers. The angle between fingers can be precisely controlled to quantitatively analyze the grasping pressure as a function of the finger position. The sponge ball is used as an object, and it exerts different pressure values at different gripping positions, as shown in Fig. 5d. Flexible pressure sensors can be used for healthcare and human motion tracking. Here, the sensor is attached to the shoe insole and is used to count the number of steps, as shown in Fig. 5e. The sensor response is fast enough to track the user's rapid walking motion (~ 100 steps/min). As the last application, the 2×2 array of the sensor can acquire not only the pressure data but also the spatial information. Figure 5f shows the sensor array and placing of objects with different weights and shapes. Such array integration allows using the developed sensor for large area pressure monitoring with sub-cm spatial resolution.

Conclusion

This work presents the design, fabrication, characterization, and application of a multi-height pressure sensor consisting of a CNT/PDMS active layer and bottom IDE. The active layer implements PDMS micropylamids fabricated using a KOH wet etched silicon as the mold. In addition, the stamp-coating of CNT ensures a robust and conformal adhesion of the CNT layer on PDMS micropylamids. The sensors with varying sizes of micropylamids are fabricated and tested over a loading range up to 100 kPa. The results indicate that the integration of multi-height micropylamids affects measurement sensitivity and detection range. The developed sensor exhibits good durability and a response time of 20 ms. The sensor can measure grasping pressure when attached to a robotic gripper. In addition, the sensor successfully tracks the walking motion at different step rates. This study shows the optimized combination of multi-height microstructures for flexible pressure sensors to fine-tune the sensor properties without replacing the sensor materials or changing the sensing scheme.

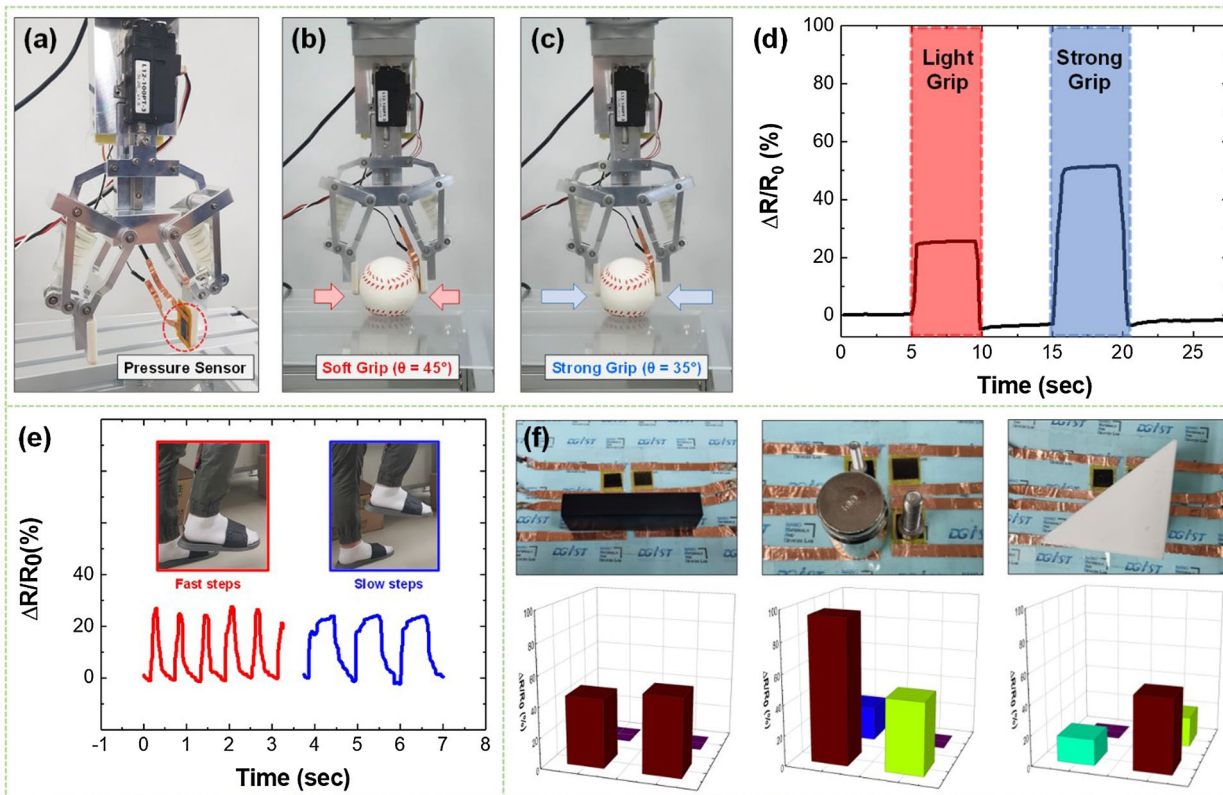


Fig. 5 a–d Gripper integration test with a light grip and strong grip. e Insole attaching test with fast step and slow step. f Array test with different weights and shapes of structures

Acknowledgements

Not applicable.

Author contributions

DOh: experiment, data curation, formal analysis, writing—original draft; JS: formal analysis, writing—original draft; HGK, CR: data curation, device fabrication; SB: experiment; SP: resources, writing—review and edit; HJK: supervision, funding acquisition, writing—review and edit. All authors read and approved the final manuscript.

Funding

This study is supported by Basic Science Research Program through the National Research Foundation of Korea (NRF), funded by the Ministry of Science and ICT of Korea (2021R1C1C1011588) and the DGIST R&D Program of the Ministry of Science and ICT of Korea (22-RT-01; 22-HRHR-05).

Availability of data and materials

All data generated or analyzed during this study are included in this published article.

Declarations**Ethics approval and consent to participate**

Not applicable.

Consent for publication

Not applicable.

Competing interests

The authors declare that they have no competing interests.

Author details

¹Department of Robotics and Mechatronics Engineering, Daegu Gyeongbuk Institute of Science & Technology (DGIST), 333, Techno jungang-daero, Hyeonpung-eup, Dalseong-gun, Daegu 42988, Republic of Korea. ²Robotics and Mechatronics Center, DGIST, Daegu 42988, Korea.

Received: 28 April 2022 Accepted: 2 June 2022

Published online: 10 June 2022

References

1. Sepúlveda A et al (2011) Nanocomposite flexible pressure sensor for biomedical applications. *Procedia Eng* 25:140–143
2. Someya T et al (2005) Conformable, flexible, large-area networks of pressure and thermal sensors with organic transistor active matrixes. *Proc Natl Acad Sci* 102(35):12321–12325
3. Someya T, Sekitani T, Iba S, Kato Y, Kawaguchi H, Sakurai T (2004) A large-area, flexible pressure sensor matrix with organic field-effect transistors for artificial skin applications. *Proc Natl Acad Sci* 101(27):9966–9970
4. Wang L, Ding T, Wang P (2009) Thin flexible pressure sensor array based on carbon black/silicone rubber nanocomposite. *IEEE Sens J* 9(9):1130–1135
5. Wan Y, Wang Y, Guo CF (2017) Recent progresses on flexible tactile sensors. *Materials Today Physics* 1:61–73
6. Zang Y, Zhang F, Di C-A, Zhu D (2015) Advances of flexible pressure sensors toward artificial intelligence and health care applications. *Mater Horiz* 2(2):140–156
7. He J et al (2020) Recent advances of wearable and flexible piezoresistive pressure sensor devices and its future prospects. *J Materomics* 6(1):86–101
8. Xu F et al (2018) Recent developments for flexible pressure sensors: a review. *Micromachines* 9(11):580
9. Chen W, Yan X (2020) Progress in achieving high-performance piezoresistive and capacitive flexible pressure sensors: a review. *J Mater Sci Technol* 43:175–188
10. Li G, Chen D, Li C, Liu W, Liu H (2020) Engineered microstructure derived multi-height deformation of flexible pressure sensor induces a supersensitive piezoresistive property in broad pressure range. *Advanced Science* 7(18):2000154
11. Wang X-M et al (2021) Sea urchin-like microstructure pressure sensors with an ultra-broad range and high sensitivity. *Nat Commun* 12(1):1–9
12. Park J et al (2018) Tailoring force sensitivity and selectivity by microstructure engineering of multidirectional electronic skins. *NPG Asia Materials* 10(4):163–176
13. Pyo S, Lee J, Kim W, Jo E, Kim J (2019) Multi-layered, multi-height fabric-based tactile sensors with high sensitivity and linearity in ultrawide pressure range. *Adv Func Mater* 29(35):1902484
14. Sang Z, Ke K, Manas-Zloczower I (2019) Design strategy for porous composites aimed at pressure sensor application. *Small* 15(45):1903487
15. Ruth SRA, Feig VR, Tran H, Bao Z (2020) Microengineering pressure sensor active layers for improved performance. *Adv Func Mater* 30(39):2003491
16. Xu M, Gao Y, Yu G, Lu C, Tan J, Xuan F (2018) Flexible pressure sensor using carbon nanotube-wrapped polydimethylsiloxane microspheres for tactile sensing. *Sens Actuators, A* 284:260–265
17. Choong CL et al (2014) Highly stretchable resistive pressure sensors using a conductive elastomeric composite on a micropillar array. *Adv Mater* 26(21):3451–3458
18. Ma C et al (2020) Robust flexible pressure sensors made from conductive micropillars for manipulation tasks. *ACS Nano* 14(10):12866–12876
19. Lian Y, Yu H, Wang M, Yang X, Zhang H (2020) Ultrasensitive wearable pressure sensors based on silver nanowire-coated fabrics. *Nanoscale Res Lett* 15(1):1–8
20. Tang X et al (2019) Multilevel microstructured flexible pressure sensors with ultrahigh sensitivity and ultrawide pressure range for versatile electronic skins. *Small* 15(10):1804559
21. Su B, Gong S, Ma Z, Yap LW, Cheng W (2015) Mimosa-inspired design of a flexible pressure sensor with touch sensitivity. *Small* 11(16):1886–1891
22. Shi J et al (2018) Multiscale multi-height design of a flexible piezoresistive pressure sensor with high sensitivity and wide linearity range. *Small* 14(27):1800819
23. Peng S, Blanloeil P, Wu S, Wang CH (2018) Rational design of ultrasensitive pressure sensors by tailoring microscopic features. *Adv Mater Interfaces* 5(18):1800403
24. Khalili N, Shen X, Naguib H (2018) An interlocked flexible piezoresistive sensor with 3D micropillar structures for electronic skin applications. *Soft Matter* 14(33):6912–6920
25. Sun Q-J et al (2018) Highly sensitive and ultrastable skin sensors for bio-pressure and bioforce measurements based on multi-height microstructures. *ACS Appl Mater Interfaces* 10(4):4086–4094

Publisher's Note

Springer Nature remains neutral with regard to jurisdictional claims in published maps and institutional affiliations.

Submit your manuscript to a SpringerOpen[®] journal and benefit from:

- Convenient online submission
- Rigorous peer review
- Open access: articles freely available online
- High visibility within the field
- Retaining the copyright to your article

Submit your next manuscript at ► [springeropen.com](https://www.springeropen.com)